Forward hadron production in ultraperipheral proton–heavy-ion collisions at the LHC and RHIC

Gaku Mitsuka

Università degli Studi di Firenze and INFN Sezione di Firenze,
Via Sansone 1, 50019 Sesto Fiorentino (Fi), Italy

E-mail: gaku.mitsuka@cern.ch

ABSTRACT: We discuss hadron production in the forward rapidity region in ultraperipheral proton–lead collisions at the LHC and proton–gold collisions at RHIC. Our discussion is based on the Monte Carlo simulations of the interactions of virtual photons emitted by a fast moving nucleus with a proton beam. We simulate the virtual photon flux with the STARLIGHT event generator and then particle production with the SOPHIA, DPMJET, and PYTHIA event generators. We show the rapidity distributions of charged and neutral particles, and the momentum distributions of neutral pions and neutrons at forward rapidities. According to the Monte Carlo simulations, we find large cross sections of ultraperipheral collisions for particle production especially in the very forward region, leading to substantial background contributions to investigations of collective nuclear effects and spin physics. Finally we can distinguish between proton–nucleus inelastic interactions and ultraperipheral collisions with additional requirements of either of the charged particles at midrapidity and a certain level of activities at negative forward rapidity.

Contents

1   Introduction

High-energy proton–nucleus ($p+A$) collisions can be classified into the following two categories according to the impact parameter b. In the first category, $p+A$ collisions occur with geometrical overlap of the colliding proton and nucleus, where the impact parameter is smaller than the sum of the radii of each particle, namely, $b < R_p + R_A$ (R_p and R_A are the radius of the proton and nucleus, respectively.) The second category is characterized by the impact parameter exceeding the sum of the two radii, $b > R_p + R_A$; thus, there is no obvious overlap between the colliding particles. Therefore, hadronic interactions mostly disappear. Nevertheless, virtual photons emitted by the relativistic nucleus may collide with the proton beam. This is called ultraperipheral collision (UPC, see ref. [1] for a review).

The use of UPCs has so far been addressed in the determination of the gluon distribution in protons and nuclei. For example, photoproduction of quarkonium in ultraperipheral $p+A$ collisions can be a probe to high, or possibly saturated, parton density in protons at small Bjorken-x (i.e., small parton momentum fraction of the momentum of protons). There indeed exist measurements of exclusive J/ψ photoproduction at the CERN Large Hadron Collider (LHC), namely, $p+\mathrm{Pb} \rightarrow p+\mathrm{Pb}+J/\psi$ [2]. Conversely, particle production in general photon–proton interactions, i.e., $\gamma+p \rightarrow X$, in UPCs has also been taken into account in the investigation of collective nuclear effects, because a large cross section of UPCs is expected, and it then provides significant background events to pure $p+A$ inelastic interaction events (hereafter "hadronic interaction", unless otherwise noted) utilized for such investigations. Indeed, a sizable cross section was found for

hadron production in ultraperipheral $d+$Au collisions [3]. It amounts to $\sim 10\,\%$ of the $d+$Au inelastic cross section.

In this paper, we discuss the effects of particle production by the $\gamma+p$ interaction in ultraperipheral $p+A$ collisions relative to the measurements of hadronic interactions, especially in forward rapidity regions at the LHC and the BNL Relativistic Heavy Ion Collider (RHIC). Concerning proton–lead ($p+$Pb) collisions at $\sqrt{s_{NN}}=5.02\,\text{TeV}$ at the LHC, we perform the calculations assuming the measurements of π^0's and neutrons with the LHCf detector [4], which originally aims at a study of nuclear effects using hadronic interaction events in a very forward region. For the case at RHIC, we consider prospective proton–gold ($p+$Au) collisions at $\sqrt{s_{NN}}=200\,\text{GeV}$ in the year 2015. In particular, the PHENIX experiment proposes a study on partonic processes in nuclei using forward prompt photons, where decayed photons from π^0's (from both the hadronic interaction and UPCs) would be dominant background events [5]. Furthermore, the measurements of the hadronic-interaction-induced prompt photons and π^0's in transversely polarized $p+$Au collisions may provide key information on the yet unestablished contributions of Sivers and Collins effects to the single spin asymmetry [5]. Our discussion on forward hadron production is based on the Monte Carlo (MC) simulations. The MC simulation for UPCs consists of two steps; the virtual photon flux is simulated by the STARLIGHT event generator [6, 7] and then the subsequent particle production in $\gamma+p$ interactions is simulated by the SOPHIA [8, 9], DPMJET [10, 11], and PYTHIA [12, 13] event generators. The MC simulation for hadronic interactions is performed by the DPMJET alone.

This paper is organized as follows. First, in section 2, the methodology of the Monte Carlo simulations is explained. Next, in section 3, we discuss the simulation results in terms of the rapidity and momentum distributions, where the hadron production in UPCs is compared with that by hadronic interactions. Additionally, we attempt reductions of UPC events by requiring associated particles. We conclude the study in this paper in section 4.

2 Methodology of Monte Carlo simulations

The MC simulation for UPCs in this study consists of two steps. First, we simulate the virtual photon flux as a function of the photon energy and impact parameter by using STARLIGHT [6]. Next, the simulation of the $\gamma+p$ interaction is performed by using SOPHIA [8] at low energy and either DPMJET [10] or PYTHIA [12] at high energy. The methodology of the MC simulation for UPCs is explained in the following subsections from 2.1 to 2.3. Conversely, the MC simulation for hadronic interactions is simply performed by using DPMJET, which will be explained in section 2.4.

2.1 Simulation of the virtual photon flux

The energy spectrum of the virtual photons emitted by the relativistic nucleus follows the Weizsäcker-Williams approximation [14, 15] implemented in STARLIGHT. Double differential photon flux due to the fast moving nucleus with velocity β is written as

$$\frac{d^3N}{dE_\gamma db^2} = \frac{Z^2\alpha}{\pi^2}\frac{x^2}{E_\gamma b^2}\left(K_1^2(x) + \frac{1}{\gamma^2}K_0^2(x)\right),\tag{2.1}$$

where N is the number of the emitted photons, E_γ is the photon energy in the rest frame of the target proton, Z is the electric charge ($Z=82$ for Pb and $Z=79$ for Au), α is the fine structure

constant, $x = E_\gamma b/\gamma$ ($\gamma = \sqrt{1-\beta^2}^{-1/2}$ is the Lorentz factor), and K_0 and K_1 are the modified Bessel functions. In the case of a relativistic nucleus ($\gamma \gg 1$), the contribution of the term $K_0^2(x)/\gamma^2$ in eq. (2.1) is safely disregarded, and indeed STARLIGHT considers only the term $K_1^2(x)$. For heavy nuclei with a large radius, the virtuality of the photon $|q^2| < (1/R_A)^2$ can be neglected; the photons are then regarded as real photons in the simulation in this analysis.

The probability P_{UPC} for an interaction of a single photon with a proton in UPCs as a function of E_γ and b is given by

$$P_{\mathrm{UPC}}(E_\gamma, b) = \frac{d^3N}{dE_\gamma db^2}\sigma_{\gamma+p\to X}(E_\gamma)\overline{P_{\mathrm{had}}}(b),\tag{2.2}$$

where $\sigma_{\gamma+p\to X}(E_\gamma)$ is the total cross section of interactions of a single real photon with a proton and $\overline{P_{\mathrm{had}}}(b)$ is the probability of having no hadronic interactions in $p+A$ collisions.

In this study, we take $\sigma_{\gamma+p\to X}(E_\gamma)$ at $\sqrt{s} < 7\,\mathrm{GeV}$ ($\sqrt{s}$ is the photon–proton center-of-mass energy) from the compilation of present experimental results [16]. A linear interpolation is performed for the estimation at a given energy between each data point. The cross section at the exact photopion production threshold $E_\gamma = 0.15\,\mathrm{GeV}$, in which no experimental measurement is present, is artificially set to zero. At $\sqrt{s} \geq 7\,\mathrm{GeV}$, $\sigma_{\gamma+p\to X}(E_\gamma)$ is taken from the best COMPETE fit results [16].

The probability of having no hadronic interactions $\overline{P_{\mathrm{had}}}(b)$ is introduced to implement the smooth cut off near the impact parameter $b = R_p + R_A$. $\overline{P_{\mathrm{had}}}(b)$ is calculated from the Woods-Saxon nuclear density and the Glauber model [6].

The range of the impact parameter b considered in the simulation is from $b^{\mathrm{min}} = 4\,\mathrm{fm}$ to $b^{\mathrm{max}} = 10^5\,\mathrm{fm}$. b^{min} is well below the sum of the effective radii of colliding particles ($\sim 8\,\mathrm{fm}$ for both $p+\mathrm{Pb}$ and $p+\mathrm{Au}$ collisions), and $\overline{P_{\mathrm{had}}}(b)$ rapidly approaches zero below $8\,\mathrm{fm}$. The photon energy in the simulation ranges from slightly above the photopion production threshold $E_\gamma^{\mathrm{min}} = 0.16\,\mathrm{GeV}$ to E_γ^{max}. E_γ^{max} is obtained by γ/b^{min} and then amounts to $700\,\mathrm{TeV}$ for $p+\mathrm{Pb}$ collisions at the LHC and $1.1\,\mathrm{TeV}$ for $p+\mathrm{Au}$ collisions at RHIC.

2.2 Simulation of low-energy photon–proton interaction

The particle production by the interaction of a low-energy photon with a proton is simulated by the SOPHIA 2.1 event generator [8]. In SOPHIA, pion production via baryon resonances, direct pion production, and multipion production are taken into account. For the baryon resonances, the known resonances from $\Delta(1232)$ to $\Delta(1950)$ are considered with their physical parameters. The resonance decay is supposed to occur isotropically according to the phase space. Multipion productions (non-diffractive interaction) dominate at $E_\gamma \gtrsim 2\,\mathrm{GeV}$ and the fraction of this interaction increases with energy. Multipion productions are implemented based on the dual parton model [17]. The SOPHIA model is used for the UPC simulations, with the photon energy ranging from E_γ^{min} to the cut off energy E_γ^{cut}.

2.3 Simulation of high-energy photon–proton interaction

At the photon energy $E_\gamma > E_\gamma^{\mathrm{cut}}$, we perform the simulation of $\gamma+p$ interactions by using either PYTHIA 6.428 or DPMJET 3.05.

In PYTHIA [12], high-energy photon interactions with a proton are classified into three different schemes [18]. Direct events describe the bare photon interaction with a parton from the proton, typically leading to high transverse-momentum (p_T) jets. In vector meson dominance (VMD) events, the photon fluctuates into a vector meson and then the vector meson interacts with the proton. This class includes low-p_T events. Finally, generalized VDM events are the interaction of a $q\bar{q}$ pair fluctuated from the photon with a parton from the proton. PYTHIA requires a simulated event that has a center-of-mass energy larger than $10\,\text{GeV}$. Thus, the cut off photon energy for the rest proton target in this study is set as $E_\gamma^{\text{cut}} = 55\,\text{GeV}$, namely, SOPHIA and PYTHIA are employed for the simulation of a $\gamma + p$ interaction for the photon energy below and above $55\,\text{GeV}$, respectively.

DPMJET [10] is based on the two-component dual parton model. Photon–proton interactions are especially implemented in the PHOJET MC event generator [19] inside DPMJET. In PHOJET, the physical photon is described as a superposition of the bare photon and virtual hadronic photon. The bare photon directly interacts with partons from the proton. The virtual hadronic photon first fluctuates into a $q\bar{q}$ pair and then hadronically interacts with the proton. DPMJET requires $E_\gamma^{\text{cut}} > 6\,\text{GeV}$, which equals to the lowest energy guaranteed by the model. Thus, SOPHIA and DPMJET are employed for the simulation of a $\gamma + p$ interaction for the photon energy below and above $6\,\text{GeV}$, respectively.

In summary, we have two types of UPC simulations: the first one is the simulations of photo-hadron production performed by SOPHIA and PYTHIA with the cut off energy $E_\gamma^{\text{cut}} = 55\,\text{GeV}$, and the second one is performed by SOPHIA and DPMJET with $E_\gamma^{\text{cut}} = 6\,\text{GeV}$.

2.4 Simulation of hadronic interaction

In the study of this paper, the DPMJET generator is used for the MC simulation of hadronic interactions, which include non-diffractive and diffractive interactions but do not include elastic scattering. The multiple scattering process in the interaction with a nuclear target, which causes nuclear shadowing, is described by the Gribov-Glauber model [20, 21] in terms of the multiple pomeron exchange. Some of the parameters for the soft particle production, which are hardly calculated by the collision theory, are determined to reproduce the experimental results. The Fermi momenta of the nucleons in the nucleus are taken into account.

3 Predictions for the ultraperipheral collisions at the LHC and RHIC

3.1 Total cross sections

The total cross section of UPCs (σ_{UPC}) is calculated by integrating eq. (2.2) over E_γ and b:

$$\sigma_{\text{UPC}} = 2\pi \int_{b^{\text{min}}}^{b^{\text{max}}} \int_{E_\gamma^{\text{min}}}^{E_\gamma^{\text{max}}} \frac{d^3N}{dE_\gamma db^2} \sigma_{\gamma+p\rightarrow X}(E_\gamma) \overline{P_{\text{had}}}(b) \, b \, db \, dE_\gamma. \tag{3.1}$$

As discussed in section 2.1, eq. (2.1) and $\overline{P_{\text{had}}}(b)$ are obtained by using STARLIGHT and $\sigma_{\gamma+p\rightarrow X}(E_\gamma)$ is taken from the experimental measurements and best fit result to these measurements; thus, eq. (3.1) is independent of the other event generators: SOPHIA, DPMJET, and PYTHIA. The calculated cross sections σ_{UPC} at the LHC and RHIC are summarized in table 1. For reference, the cross sections for $p + A$ inelastic interactions are presented, which are calculated by using DP-MJET. We find the sizable σ_{UPC}'s, which amount to $20\,\%$ and $9\,\%$ of the hadronic cross sections at

Table 1. Cross sections for particle production in ultraperipheral collisions and hadronic interactions.

	UPC (mb)			Hadronic interaction (mb)		
	Total	π^0	n	Inelastic	π^0	n
LHC ($p+$Pb collisions at $\sqrt{s_{NN}} = 5.02\,$TeV)	434	78	153	2189	91	125
RHIC ($p+$Au collisions at $\sqrt{s_{NN}} = 200\,$GeV)	170	9	73	1851	67	35

the LHC and RHIC, respectively. Effective cross sections that require the forward π^0 and neutron tagging will be discussed in section 3.3.

3.2 Rapidity distributions

The charged and neutral particle pseudorapidity (η_{lab}) distributions in the detector reference frame are shown in figure 1. The solid curves indicate the UPC simulation events generated by using SOPHIA at low energy and DPMJET at high energy. The dashed curves indicate the UPC simulation events created by using SOPHIA at low energy and PYTHIA at high energy. Dotted curves indicate the predictions of $p+A$ inelastic events with DPMJET. Hereafter, the directions of the moving proton and the nucleus are assumed to be positive and negative rapidities, respectively. Particle productions in UPCs are clearly distributed around positive forward rapidities because of the Lorentz boost by the proton beam. It should be noted that the cross sections of UPCs exceed those of hadronic inelastic interactions for the charged and neutral particles at $\eta_{\mathrm{lab}} > 9$ at the LHC and $\eta_{\mathrm{lab}} > 7$ at RHIC, respectively. This indicates that contamination of background UPC events could spoil the investigations of collective nuclear effects and spin physics carried out with the measurements of hadronic interactions in such rapidity regions.

3.3 Transverse and longitudinal momentum distributions

The simulated p_{T} and longitudinal momentum fraction (z, defined as $p_z/p_{z\,\mathrm{max}}$) distributions for the π^0 and neutron productions at the positive forward rapidities, the direction of the proton remnant, are shown in figure 2 for the LHC and in figure 3 for RHIC.

For the distributions at the LHC, we choose the rapidity regions in the detector reference frame $8.5 < y_{\mathrm{lab}} < 11.0$ for π^0's and $7.0 < y_{\mathrm{lab}} < 9.05$ for neutrons, which roughly correspond to the acceptance of the LHCf detector [4]. The LHCf experiment provides an opportunity to investigate the effects of high parton density on forward hadron production, which emerge as a suppression in the momentum distributions in $p+$Pb inelastic interactions relative to that in $p+p$ inelastic interactions. However, the π^0 and neutron productions in UPCs may give background events to these measurements and spoil the analysis sensitivity [22]. In the left top and left bottom panels of figure 2, the p_{T} distributions of π^0's and neutrons in UPCs, respectively, have a steep peak at $p_{\mathrm{T}} \approx 0.2\,$GeV. These peaks originate in the channels $\gamma + p \to \pi^0 + p$ and $\gamma + p \to \pi^+ + n$ via baryon resonances, and these channels dominate at the E_γ region from E_γ^{min} to $0.5\,$GeV, in which the photon flux is larger than that at higher E_γ. Consequently, the double differential cross sections of UPCs exceed those of hadronic interactions at $p_{\mathrm{T}} \approx 0.2\,$GeV. The dominance of the channel $\gamma + p \to \pi^+ + n$ in UPCs is also clearly found in the right bottom panel of figure 2. Forward neutrons produced in UPCs have a larger z value; low momentum neutrons produced by a low-energy $\gamma + p$ interaction in the proton's rest frame are boosted to nearly the same velocity of the
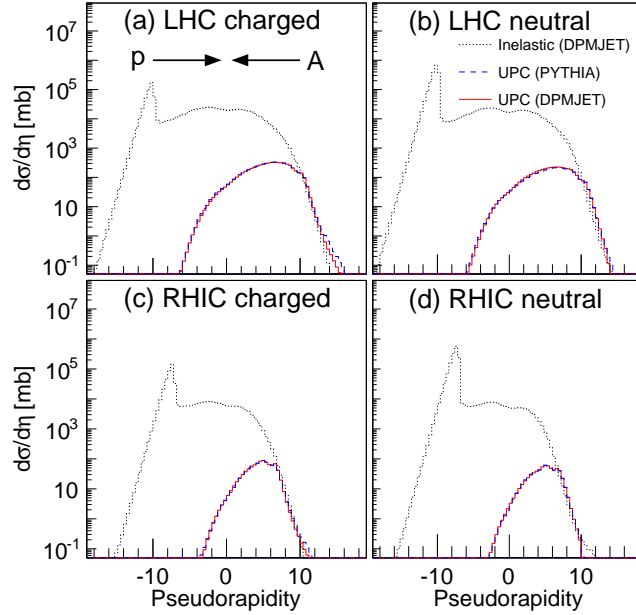
Figure 1. Charged (left) and neutral particle (right) pseudorapidity distributions at the LHC (top) and RHIC (bottom), respectively. The solid curves and dashed curves indicate the UPC simulation events generated by using STARLIGHT+SOPHIA+DPMJET and STARLIGHT+SOPHIA+PYTHIA, respectively. The dotted curves indicate the simulated $p+A$ inelastic events with DPMJET.

projectile proton. As also inferred in section 3.2, we see that the presence of UPCs certainly provides a significant background contribution to the study on collective nuclear effects.

The p_T and z distributions for π^0 and neutron productions at RHIC are shown in figure 3. We choose the rapidity regions $3.1 < y_{lab} < 3.8$ for π^0's and $4.0 < y_{lab} < 5.4$ for neutrons, which especially correspond to the acceptance of the MPC-EX detector [5] and zero-degree calorimeter [23] of the PHENIX experiment, respectively. The prompt photon measurements with the MPC-EX detector in $p+$Au collisions could provide key information on partonic processes in the Au nucleus, whereas the photons decayed from π^0's, produced by both hadronic interactions and UPCs, could be the dominant background events. The p_T distributions of π^0's of the UPCs have almost the same shapes as those of the hadronic interactions (the upper left panel), while the absolute yield is at most 3 % of the hadronic interactions. Thus, we conclude that the UPCs provide a negligible contribution to the amount of π^0's, which leads to the background decayed photon events. The z distribution of π^0's of the UPCs (the upper right panel) is slightly steeper than the hadronic interactions, and the absolute yield is again negligible. Conversely, neutron productions of the UPCs compete with those of hadronic interactions at $p_T \lesssim 0.2$ GeV. This can be explained by the same mechanism as found in figure 2, namely, dominance of the channel $\gamma + p \to \pi^+ + n$ via baryon resonances in UPCs. The z distribution of neutrons has a similar shape, as shown in the right bottom panel of figure 2. Concerning the measurements of forward prompt photons and hadrons in polarized $p+$Au collisions, which are sensitive to the origin of spin asymmetry [24], we also confirm that the UPC contribution to the total amounts of prompt photons and π^0's is negligible, while the equivalent amount of UPC contributions as well as of hadronic interactions is found for neutrons.
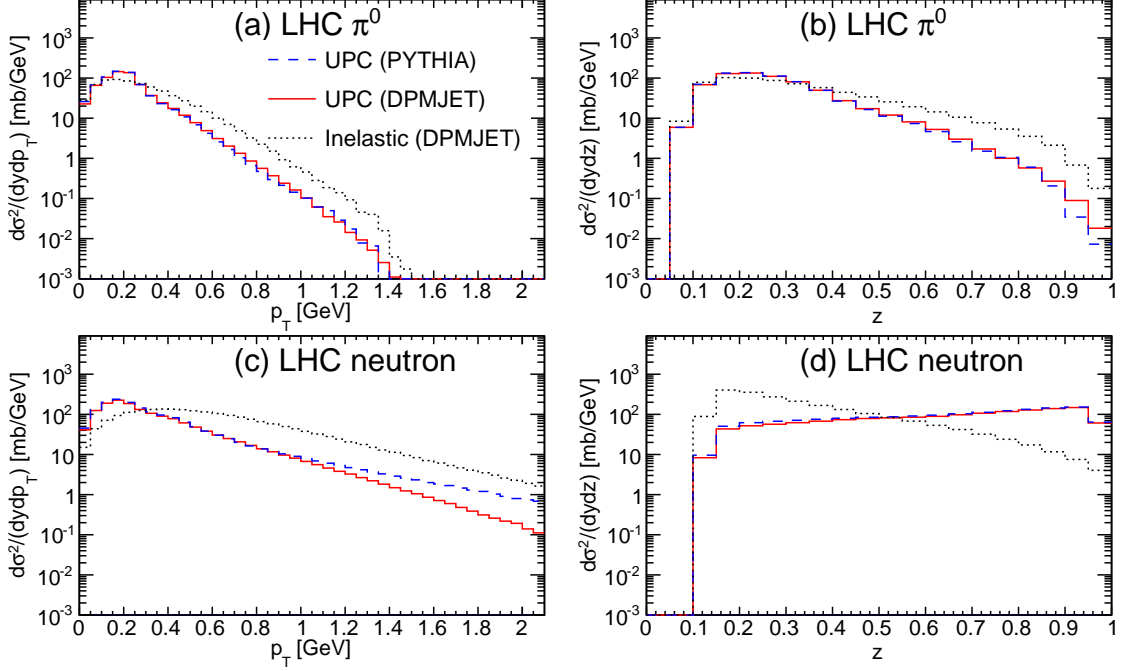
Figure 2. Simulated p_T and z spectra for π^0's and neutrons in $p+$Pb collisions at the LHC. The solid curves and dashed curves indicate the UPC simulation events generated by using STARLIGHT+SOPHIA+DPMJET and STARLIGHT+SOPHIA+PYTHIA, respectively. The dotted curves indicate the simulated $p+$Pb inelastic events with DPMJET.

We tested at both the LHC and RHIC a possible dependence of the p_T and z distributions on the cut off energy $E_\gamma^{\rm cut}$. The comparison of the two distributions at the LHC, with one based on the UPC simulations with DPMJET above $E_\gamma^{\rm cut} = 6\,{\rm GeV}$ and the other based on the UPC simulations with DPMJET above $E_\gamma^{\rm cut} = 55\,{\rm GeV}$, provides negligible differences between these two distributions relative to the differences between DPMJET and PYTHIA. The comparison at RHIC shows larger differences than at the LHC; nevertheless it is at the same level with the differences between DPM-JET and PYTHIA. Additionally, we mention the difference on the p_T distribution between DPMJET and PYTHIA; this is dominantly caused by the different values of the minimum p_T for the multiple interactions (i.e., hard scatterings) employed in each model.

Now, we turn back to table 1. The effective cross sections of π^0 and neutron productions are defined as the cross sections having at least one π^0 or neutron hitting within the rapidity ranges focused on above. We find that the UPC cross sections are compatible or larger than the hadronic cross sections, except for π^0's at RHIC. It should be noted that the effective cross section involves the simulations of specific hadron production and is then no longer independent of the hadronic interaction event generators. The values in table 1 for UPCs are especially calculated by using STARLIGHT, SOPHIA, and DPMJET, and those for hadronic interactions are calculated by using DPMJET. Nevertheless, the essential conclusion will not change depending on the choice of event generators.
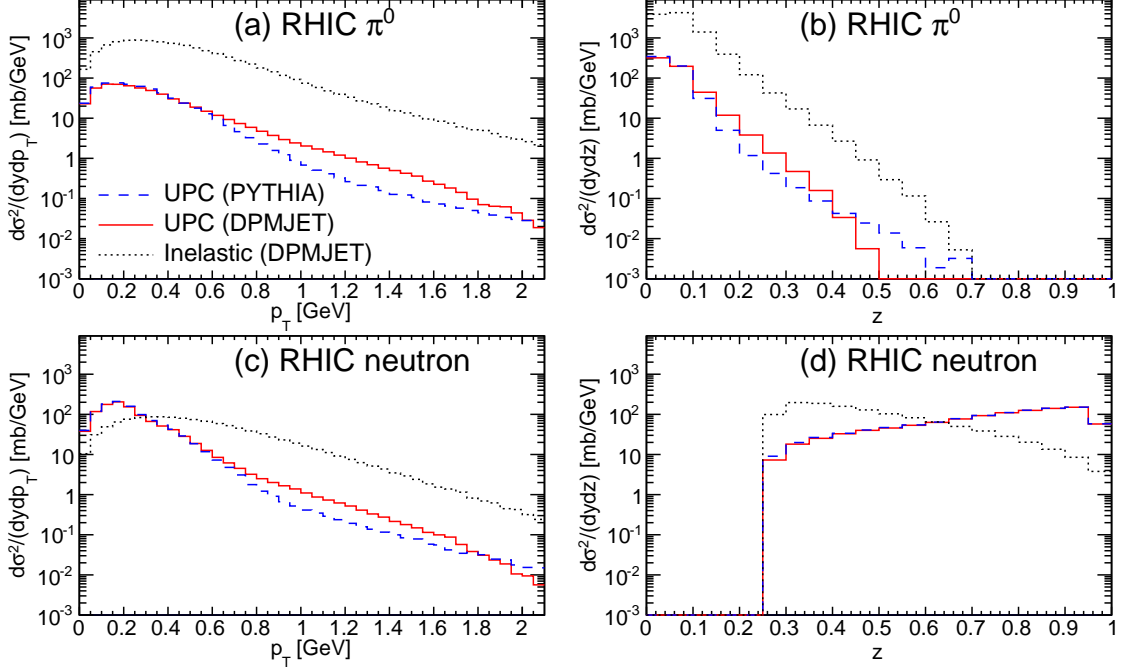
Figure 3. Simulated p_T and z spectra for π^0's and neutrons in $p + $Au collisions at RHIC. The solid curves and dashed curves indicate the UPC simulation events generated by using STARLIGHT+SOPHIA+DPMJET and STARLIGHT+SOPHIA+PYTHIA, respectively. The dotted curves indicate the simulated $p + $Au inelastic events with DPMJET.

3.4 Reduction of the contribution of the ultraperipheral collisions

As seen in figure 1, the particle productions in UPCs are distributed in forward rapidity regions, whereas those in the hadronic interactions achieve a plateau at midrapidity and also have a large number of spectator nucleons at $\eta_{\mathrm{lab}} \sim -8$. Such differences in the rapidity distributions between UPCs and hadronic interactions can be utilized to separate these two components.

First, we investigate a separation capability by requiring some activities in the midrapidity region. The following cuts are applied to π^0's and neutrons to eliminate the UPC induced events as well as to ensure that the hadronic interaction events remain unchanged: (1) number of charged particles is greater than 2, (2) the charged particles have $p_T > 0.2\,$GeV, and (3) the charged particles have rapidity $|\eta_{\mathrm{lab}}| < 2.5$ at the LHC and $|\eta_{\mathrm{lab}}| < 0.35$ at RHIC. The rapidity regions focused on in the cuts correspond to the rapidity ranges of the ATLAS and PHENIX inner detectors [25, 26].

Figure 4 shows the p_T distributions after the cuts at the LHC and RHIC. The absolute yields of the UPCs at the LHC (RHIC) are reduced to less than 60 % (8 %) for π^0's and 40 % (10 %) for neutrons, although the absolute yields of hadronic interactions are kept to be larger than, at most, 85 % (50 %) for π^0's and 85 % (20 %) for neutrons. Consequently, these cuts with the charged particles at midrapidity constrain the relative yields of the UPCs to the hadronic interactions by, at most, 15 % (0.2 %) for π^0's and 25 % (1.5 %) for neutrons. However, the cuts still leave the remaining contributions of the UPCs and unavoidably reduce hadronic interaction events. It should also be noted that the rejected hadronic interaction events are mostly single and double diffractive events, generally providing a small number of charged particles at midrapidity, although the reduction efficiency of
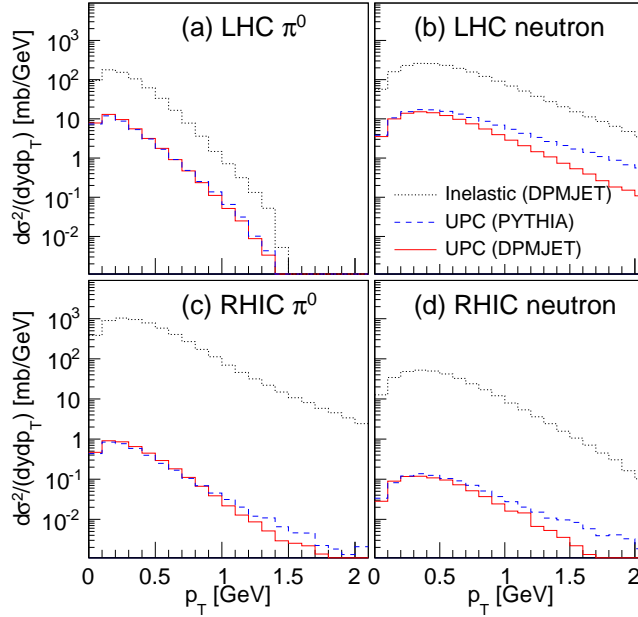
Figure 4. Simulated p_T and z spectra for π^0's and neutrons with the cuts applied at the LHC and RHIC (see text in detail). The solid curves and dashed curves indicate the UPC simulation events generated by using STARLIGHT+SOPHIA+DPMJET and STARLIGHT+SOPHIA+PYTHIA, respectively. The dotted curves indicate the simulated $p+A$ inelastic events with DPMJET.

$10\% - 50\%$ highly depends on the forward π^0 and neutron energies.

Next, we test more sharp cuts, which require an activity in the negative very forward region and which can be identified by a zero-degree calorimeter. In this rapidity region, only hadronic interactions produce a large number of spectator nucleons fragmented from the colliding nucleus. Each nucleon has an approximate energy of $1.58\,\mathrm{TeV}$ at the LHC and $100\,\mathrm{GeV}$ at RHIC. The cuts applied to the simulated events consist of three requirements: (1) the number of neutrons is greater than 1 (note that a proton can be swept away by the magnets located between an interaction point and a detection point, and thus no proton reaches the detector), (2) the neutrons have $E > 1\,\mathrm{TeV}$ at the LHC and $E > 50\,\mathrm{GeV}$ at RHIC, and (3) the neutrons have rapidity $\eta_{\mathrm{lab}} < -6.5$. The rapidity region $\eta_{\mathrm{lab}} < -6.5$ roughly corresponds to the acceptance of the zero-degree calorimeter located in the nucleus remnant side. Consequently, the contribution of UPCs is perfectly eliminated by these cuts, although that of the hadronic interactions is unchanged.

According to the discussions above, we conclude that a reduction in the contributions from UPCs to the measurements of forward hadrons is certainly feasible with requirements of some activities in mid and forward rapidity regions. In particular, we expect a stringent reduction if we detect spectator nucleons, for example, with a zero-degree calorimeter, at negative rapidity $\eta_{\mathrm{lab}} \lesssim -6.5$.

4 Conclusions

We discussed hadron production in forward rapidity regions by ultraperipheral $p+\mathrm{Pb}$ collisions at the LHC and $p+\mathrm{Au}$ collisions at RHIC. Our discussion was based on the MC simulations

of the interaction of the virtual photons emitted by a fast moving nucleus with a proton, which consisted of several event generators: STARLIGHT, SOPHIA, DPMJET, and PYTHIA. We found large cross sections for particle production in the very forward region, leading to a substantial background contribution to the measurements of hadronic interactions at both the LHC and RHIC. Therefore, the presence of UPCs had to be taken into account in the analyses on the investigation of collective nuclear effects and spin physics in order to correctly evaluate the fraction of the hadronic cross section relative to the measured cross section. We tested two types of cuts to reduce the fraction of UPCs relative to hadronic interactions; one required charged particles at midrapidity, and the other required very forward spectator neutrons. The former cut certainly reduced the UPC induced events while unavoidably rejecting some hadronic events. The second cut perfectly eliminated the fraction of π^0's and neutrons produced by UPCs and had no effect on the hadronic interaction events.

Acknowledgments

References

[1] C. A. Bertulani, S. R. Klein, and J. Nystrand, *Physics of Ultra-Peripheral Nuclear Collisions*, *Ann. Rev. Nucl. Part. Sci.* **55** (2005) 271-310.

[2] ALICE Collaboration, *Exclusive J/ψ Photoproduction off Protons in Ultraperipheral p–Pb Collisions at $\sqrt{s_{NN}} = 5.02\,TeV$*, *Phys. Rev. Lett.* **113** (2014) 232504.

[3] V. Guzey and M. Strikman, *Electromagnetic and strong contributions to dAu soft coherent inelastic diffraction at the BNL Relativistic Heavy Ion Collider (RHIC)*, *Phys. Rev.* **C 77** (2008) 067901.

[4] LHCf Collaboration, *LHCf Technical Design Report*, CERN-LHCC-2006-004 (unpublished).

[5] PHENIX Collaboration, S. Campbell et al., *A Proposal for the Muon Piston Calorimeter Extension (MPC-EX) to the PHENIX Experiment at RHIC*, arXiv:1301.1096.

[6] S. R. Klein and J. Nystrand, *Exclusive vector meson production in relativistic heavy ion collisions*, *Phys. Rev.* **C 60** (1999) 014903.

[7] STARLIGHT webpage, https://starlight.hepforge.org/.

[8] A. Mücke, R. Engel, J.P. Rachen, R.J. Protheroe and T. Stanev, *Monte Carlo simulations of photohadronic processes in astrophysics*, *Comput. Phys. Comm.* **124** (2000) 290-314.

[9] SOPHIA webpage, http://homepage.uibk.ac.at/~c705282/SOPHIA.html.

[10] F. W. Bopp, J. Ranft, R. Engel and S. Roesler, *Antiparticle to particle production ratios in hadron-hadron and d–Au collisions in the DPMJET-III Monte Carlo model*, *Phys. Rev.* **C 77** (2008) 014904.

[11] DPMJET webpage, http://sroesler.web.cern.ch/sroesler/dpmjet3.html.

[12] T. Sjöstand, S. Mrenna and P. Skands, *PYTHIA 6.4 physics and manual*, *JHEP* **05** (2006) 026.

[13] PYTHIA 6.4 webpage, http://pythia6.hepforge.org/.

[14] C. von Weizsäcker, *Radiation emitted in collisions of very fast electrons*, *Z. Physik* **88** (1934) 612-625.

[15] E. J. Williams, *Nature of the high-energy particles of penetrating radiation and status of ionization and radiation formulae*, *Phys. Rev.* **45** (1934) 729-730.

[16] K. A. Olive et al. (Particle Data Group), *The Review of Particle Physics*, *Chin. Phys.* **C 38** (2014) 090001.

[17] A. Capella, U. Sukhatme, C-I Tan and J. Tran Thanh Van, *Dual parton model*, *Phys. Rep.* **236** (1994) 225-329.

[18] G. A. Schuler and T. Sjöstand, *The hadronic properties of the photon in γp interactions*, *Phys. Lett.* **B 300** (1993) 169-174.

[19] R. Engel, *Photoproduction within the two-component Dual Parton Model: Amplitudes and cross sections*, *Z. Phys.* **C 66** (1995) 203-214.

[20] V. N. Gribov, *Interaction of gamma quanta and electrons with nuclei at high-energies*, *Sov. Phys. JETP* **30** (1970) 709-717.

[21] R. J. Glauber and G. Matthiae, *High-energy scattering of protons by nuclei*, *Nucl. Phys.* **B 21** (1970) 135-157.

[22] LHCf Collaboration, O. Adriani et al., *Transverse-momentum distribution and nuclear modification factor for neutral pions in the forward-rapidity region in proton-lead collisions at $\sqrt{s_{NN}} = 5.02\,TeV$*, *Phys. Rev.* **C 89** (2014) 065209.

[23] PHENIX Collaboration, C. Adler et al., *The RHIC zero degree calorimeters*, *Nucl. Instrum. Meth.* **A 470** (2001) 488-499.

[24] Z-B Kang and F. Yuan, *Single spin asymmetry scaling in the forward rapidity region at RHIC*, *Phys. Rev.* **D 84** (2011) 034019.

[25] ATLAS Collaboration, *The ATLAS Experiment at the CERN Large Hadron Collider*, *JINST* **3** (2008) S08003.

[26] PHENIX Collaboration, M. Allen et al., *PHENIX inner detectors*, *Nucl. Instrum. Meth.* **A 499** (2003) 549-559.